

# Gadolinium<sup>3+</sup>-doped mesoporous silica nanoparticles as a potential magnetic resonance tracer for monitoring the migration of stem cells in vivo

Yingying Shen<sup>1,2,\*</sup>Yuanzhi Shao<sup>3,\*</sup>Haoqiang He<sup>1</sup>Yunpu Tan<sup>4</sup>Xiumei Tian<sup>2</sup>Fukang Xie<sup>2</sup>Li Li<sup>1</sup>

<sup>1</sup>Imaging Diagnostic and Interventional Center, Sun Yat-sen University Cancer Center, Guangzhou, Guangdong, China; <sup>2</sup>Department of Histology and Embryology, Zhongshan School of Medicine, Sun Yat-sen University, Guangzhou, Guangdong, China; <sup>3</sup>Key Laboratory of Optoelectronic Materials and Technologies, School of Physics and Engineering, Sun Yat-sen University, Guangzhou, Guangdong, China; <sup>4</sup>Department of Gastrointestinal Surgery, Sun Yat-sen University, Guangzhou, Guangdong, China

\*These authors contributed equally to this work

Correspondence: Li Li  
Imaging Diagnosis and Interventional Center,  
Sun Yat-sen University Cancer Center,  
651 Dongfeng East Road, Yuexiu District,  
Guangzhou, Guangdong 510060, China  
Tel +86 20 8734 3476  
Fax +86 20 8734 3476  
Email li2@mail.sysu.edu.cn

Fukang Xie  
Department of Histology and Embryology,  
Zhongshan School  
of Medicine, Sun Yat-sen University,  
74 Zhongshan Road, Yuexiu District,  
Guangzhou, Guangdong 510080, China  
Tel +86 20 6178 7376  
Fax +86 20 6178 7376  
Email frankxie2000@yahoo.com

**Abstract:** We investigated the tracking potential of a magnetic resonance imaging (MRI) probe made of gadolinium-doped mesoporous silica MCM-41 ( $Gd_2O_3@MCM-41$ ) nanoparticles for transplanted bone mesenchymal stem cells (MSCs) and neural stem cells (NSCs) in vivo. The nanoparticles, synthesized using a one-step synthetic method, possess hexagonal mesoporous structures with appropriate assembly of nanoscale  $Gd_2O_3$  clusters. They show little cytotoxicity against proliferation and have a lower effect on the inherent differentiation potential of these labeled stem cells. The tracking of labeled NSCs in murine brains was dynamically determined with a clinical 3T MRI system for at least 14 days. The migration of labeled NSCs identified by MRI corresponded to the results of immunofluorescence imaging. Our study confirms that  $Gd_2O_3@MCM-41$  particles can serve as an ideal vector for long-term MRI tracking of MSCs and NSCs in vivo.

**Keywords:** nanoparticles, gadolinium, magnetic resonance imaging, stem cells

## Introduction

Stem cell therapies have continued to capture the growing interest of the scientific community. Bone mesenchymal stem cells (MSCs) are of crucial importance, because they have the capacity to differentiate into a wide variety of cell types and thus contribute to tissue repair in various organs and systems. Transplanted MSCs can also enhance regeneration of injured cells by secreting cytokines.<sup>1,2</sup> Neural stem cell (NSC) transplantation is a leading strategy for replacing lost cells and provides neuroprotection in neurologic diseases; there are many reports on functional neurological recovery using NSC-based therapies.<sup>3-6</sup> Noninvasive imaging techniques, such as magnetic resonance imaging (MRI),<sup>7-11,12</sup> are a convenient option for analyzing the behavior of stem cells, including the biodistribution and migration of cells, which is highly promising for visual stem cell therapies.<sup>13-15</sup>

Various Gd-doped mesoporous silica biomaterials used as MRI probes have been investigated for their application in stem cell tracking. Because of its good biocompatibility, relative noncytotoxicity, and nanostructure, mesoporous silica qualifies as an ideal biomaterial for stem cell labeling. The mesoporous structure can hold paramagnetic gadolinium (Gd) ions, allowing easy water access to Gd ions and a high degree of interaction between Gd ions and water protons, which contribute to increasing MR signals.<sup>16-20</sup> Hsiao et al<sup>21</sup> first reported on an efficient stem cell-tracking media made

by Gd-loaded mesoporous silica nanoparticles that did not affect cell viability or differentiation; this laid the foundation for future visual stem cell therapies using  $T_1$ -weighted MRI with a Gd-based positive contrast agent instead of superparamagnetic iron oxide (SPIO). Additionally, monitoring the fate of transplanted cells in vivo is an increasingly indispensable part of assessing the nanoprobe as a cellular tracer; in particular, the combination of MR images with histological analysis provides for a more thorough investigation.

In our previous work, we reported the synthesis and characteristics of Gd<sup>3+</sup>-incorporated mesoporous SiO<sub>2</sub> (Gd<sub>2</sub>O<sub>3</sub>@SiO<sub>2</sub>) using a one-step synthesis method.<sup>22</sup> The mesoporous structure with tunable nanosized pores makes it an excellent platform for self-assembly of Gd<sub>2</sub>O<sub>3</sub> nanoclusters. The ultrafine Gd<sub>2</sub>O<sub>3</sub> nanoparticles have been demonstrated to be useful for MRI.<sup>23,24</sup> On the basis of this mesoporous material preparation technology, we synthesized Gd-doped mesoporous silica MCM-41 (Gd<sub>2</sub>O<sub>3</sub>@MCM-41) nanoparticles, which had better efficacy than Gd-diethylenetriaminepentacetate, and systematically investigated their biocompatibility and biodistribution.<sup>25</sup> The detailed theoretical calculation was consistent with the results of the cytotoxicity and immunotoxicity assays, which showed that Gd<sub>2</sub>O<sub>3</sub> nanoclusters or Gd ions were hardly dissociated from the mesoporous silica structure and that the Gd<sub>2</sub>O<sub>3</sub>@MCM-41 nanocomposite could be developed as a potentially safe and effective MRI contrast agent.<sup>25</sup> In this study, we investigate the effects of Gd<sub>2</sub>O<sub>3</sub>@MCM-41 on the biological characteristics of labeled MSCs and NSCs and assess their tracking potential in murine transplant models. These particles were found to have fairly low cytotoxicity against cell proliferation and had only a slight effect on the inherent differentiation potential of the labeled stem cells. Murine models indicated that Gd<sub>2</sub>O<sub>3</sub>@MCM-41 could be a suitable candidate for monitoring MSCs and NSCs.

## Materials and methods

### Materials and their sources

Cetyltrimethyl ammonium bromide (C<sub>16</sub>TAB), tetraethoxysilane (TEOS), 3-(4,5-dimethylthiazol-2-yl)-2,5-diphenyltetrazolium bromide (MTT) reagent, oil red O, alkaline phosphatase kits, alcian blue, rabbit anti- $\beta$ -tubulin III antibody, and Hoechst nuclear dye were purchased from Sigma-Aldrich (St Louis, MO, USA). GdCl<sub>3</sub>·6H<sub>2</sub>O was provided by Alfa Aesar (Ward Hill, MA, USA). Sodium carboxymethyl cellulose and polyethylene glycol were supplied by Kayon Biological Technology (Shanghai, China). Dulbecco's modified Eagle's medium (DMEM)/F12 (1:1), fetal bovine serum (FBS), basic fibroblast growth factor,

and B27 were provided by Gibco BRL (Life Technologies, Gaithersburg, MD, USA). Cy3 AffiniPure goat anti-rabbit IgG was purchased from Jackson ImmunoResearch (West Grove, PA, USA). Complete bone MSC differentiation medium was purchased from R&D Systems (Minneapolis, MN, USA). All other reagents were obtained from Sinopharm Chemical Reagent (Shanghai, China).

### Synthesis and characterization of Gd<sub>2</sub>O<sub>3</sub>@MCM-41

In a typical synthesis, 25% ammonia (2 mL) was dissolved in 100 mL deionized water, and C<sub>16</sub>TAB (0.2 g) and 1% polyethylene glycol (2 mL) were added to the mixture. The mixture was stirred at room temperature. Then, TEOS (1 mL) was added to the solution with stirring for 15 minutes, followed by the addition of GdCl<sub>3</sub>·6H<sub>2</sub>O (0.1 g). After an hour of stirring at room temperature, the precipitate was centrifuged and placed in liquid nitrogen for speed-freezing, and then the sample was placed in a lyophilizer. After it was completely dried, the sample was calcined for 5 hours (550°C) in order to obtain Gd<sub>2</sub>O<sub>3</sub>@MCM-41 nanoparticles.

Gd<sub>2</sub>O<sub>3</sub>@MCM-41 nanoparticles were dissolved in phosphotungstic acid solution and shattered by an ultrasonic cell disrupter (Scientz, Ningbo, China). Then, the solution was dripped on copper-wire grids covered with amorphous carbon film. The grids were examined with a transmission electron microscope (TEM) (JEM-2010HR; JEOL, Tokyo, Japan). Besides, a scanning electron microscope (LEO-1530VP; LEO Elektronenmikroskopie GmbH, Oberkochen, Germany) was also used to investigate the size and morphology of Gd<sub>2</sub>O<sub>3</sub>@MCM-41 nanoparticles. The compositions and the Gd concentration of Gd<sub>2</sub>O<sub>3</sub>@MCM-41 were measured by energy-dispersive X-ray spectroscopy (ISIS-300; Oxford Instruments, Abingdon, UK) and inductively coupled plasma-atomic emission spectrometry (Ciros Vision; Spectro, Kleve, Germany), respectively.

### Cell culture and cell labeling

MSCs were harvested from the bone marrow of Sprague Dawley (SD) rats (8–9 days old; Sun Yat-sen University, Guangzhou, China) and cultured in DMEM/F-12 supplemented with 10% FBS. NSCs were harvested from the hippocampus of newborn green fluorescent protein (GFP)-expressing SD rats (1–3 days old; Jinan University, Guangzhou, China) and cultured in (DMEM)/F12 supplemented with basic fibroblast growth factor (20 ng/mL) and B27 (0.1 mL/mL).

Gd<sub>2</sub>O<sub>3</sub>@MCM-41 nanoparticles were dissolved in carboxymethyl cellulose 4% (phosphate-buffered saline [PBS]) and shattered using an ultrasonic cell disrupter

(200 W, 5 minutes). MSCs were incubated with the growth medium supplemented with 10% FBS containing Gd<sub>2</sub>O<sub>3</sub>@MCM-41 for 24 hours. NSCs were induced to differentiate into neurons (described in the Differentiation of labeled cells section) and labeled with Gd<sub>2</sub>O<sub>3</sub>@MCM-41 (50 µg/mL). A TEM (FEI, Hillsboro, OR, USA) was used to observe cellular Gd<sub>2</sub>O<sub>3</sub>@MCM-41 distribution. To determine the optimal labeling concentration, MSCs labeled with 10, 20, or 50 µg/mL of Gd<sub>2</sub>O<sub>3</sub>@MCM-41 were harvested in a suspension comprising 100 µL medium in 0.2 mL Eppendorf tubes. MRI examination was performed using a 3T MRI scanner (Siemens, Munich, Germany).

## Cell viability and differentiation

Proliferation of labeled MSCs (0, 20, or 50 µg/mL Gd<sub>2</sub>O<sub>3</sub>@MCM-41) was evaluated by the MTT colorimetric assay on days 2, 4, 8, and 12. All experiments were repeated three times for statistical analysis (one-way analysis of variance).

The potential of labeled MSCs to differentiate into adipocytes, osteocytes, and chondrocytes was analyzed. For adipogenic differentiation, labeled MSCs were plated in 24-well plates at  $1.5 \times 10^4$ /well. At 100% confluency, the cells were cultured in adipogenic differentiation medium for 15 days; the medium was replaced every 3–4 days. Cells were stained with oil red O for identifying lipid droplets. For osteogenic differentiation, labeled MSCs were plated in 24-well plates at  $3.3 \times 10^3$ /well. At 70% confluency, cells were cultured in osteogenic differentiation medium for 15 days, with the medium replaced every 2–3 days. Cells were stained with alkaline phosphatase. For chondrogenic differentiation, about  $1.25 \times 10^4$  MSCs labeled with 50 µL of chondrogenic differentiation medium were resuspended in a 1.5 mL centrifuge tube and centrifuged at  $200 \times g$  for 5 minutes. The cell pellets were cultured in the tube for 18 days, with the medium replaced every 2–3 days. Cell pellets were stained with alcian blue.

For neuronal differentiation of NSCs, cells were infected with replication-deficient adenoviral (Adv) vector carrying human neurotrophin-3 (AdvNT-3) at a multiplicity of infection (MOI, plaque-forming units/cell) of 100 (NT-3-NSCs), or Adv vector carrying human TrkC (AdvTrkC) at an MOI of 150 (TrkC-NSCs) for 3 hours. Then, NT-3-NSCs and TrkC-NSCs were mixed (1:1), labeled (50 µg/mL) for 24 hours, and cultured in culture medium for 4 days. Immunocytochemical staining was performed. Briefly, labeled NSCs were fixed (2.5% paraformaldehyde, 30 minutes), blocked (goat serum, 1:10, 30 minutes, room temperature) and incubated with the primary antibody (anti-β-tubulin III antibody produced in rabbit, 1:500, 4°C) overnight and the secondary antibody

for 1 hour (Cy3 AffiniPure goat anti-rabbit IgG, 37°C). Then, labeled NSCs were incubated with Hoechst nuclear dye (30 minutes, 37°C) and viewed.

We also studied the differentiation potential of unlabeled MSCs and unlabeled NSCs as negative controls.

## In vivo imaging

Animal experiments were conducted according to the National Institutes of Health animal care and use guidelines. The experimental SD rats (250–300 g) were purchased from the animal experiment center of the Medical College, Sun Yat-sen University, Guangzhou, China.

Labeled MSCs ( $4 \times 10^6$ ) in serum-free DMEM/F-12 (100 µL) were injected intramuscularly into the left thigh. Unlabeled cells were injected into the contralateral thigh. The 3T MRI scanner was used. Labeled NSCs ( $1 \times 10^5$ ) in 20 µL of serum-free media were injected into the right hemisphere 2.0 mm lateral and 2.0 mm posterior to the bregma and 4.0 mm below the skull surface; this took 5 minutes. Unlabeled NSCs were injected into the left hemisphere. MRI experiments were performed on day 1, day 4, day 9, and day 14 after surgery. The in vivo MR experiment was repeated five times for each cell type.

## Histological analysis

After 14 days of tracking, animals were killed for histology analyses. Rats were systemically perfused with physiological saline containing 0.002% heparin, followed with 4% paraformaldehyde/PB. Brains were postfixed overnight and placed in 30% sucrose/PB. The parts of the brains that showed hyperintensity in the MR images were cut into 30 µm coronal sections.

Some frozen sections were observed directly, or stained with hematoxylin and eosin. Immunocytochemical analysis (described in the Differentiation of labeled cells section) was used to assess whether donor-labeled NSCs could survive and retain their potential for neuronal differentiation after a long time tracking.

## Results

### Structure of Gd<sub>2</sub>O<sub>3</sub>@MCM-41 nanoparticles

Figure 1A–C shows the morphology and microstructure observed at different magnifications (A), particle-size distribution (B), and composition (C) of the synthesized Gd<sub>2</sub>O<sub>3</sub>@MCM-41 silica nanoparticles. According to Figure 1A and B, the Gd<sub>2</sub>O<sub>3</sub>@MCM-41 nanoparticles consist of a monodispersed sphere around 90 nm in diameter (average

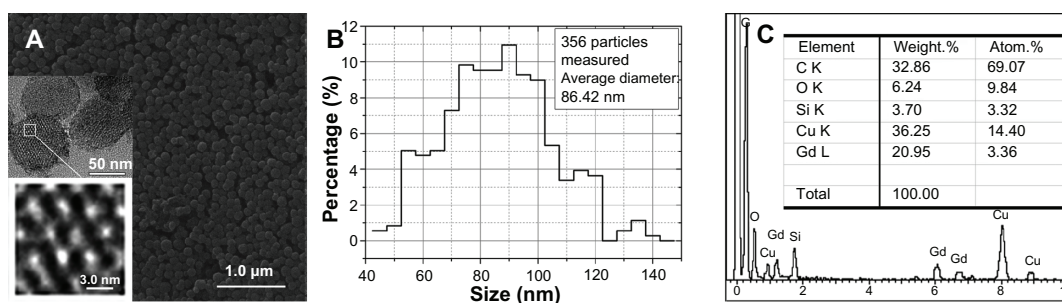


**Figure 1** (A) Electronic microscope images of the synthesized nanoparticles with a 1.55 atomic% gadolinium doping; two insets included are the magnified views of a gadolinium-doped mesoporous silica MCM-41 ( $Gd_2O_3@MCM-41$ ). (B) Size distribution of  $Gd_2O_3@MCM-41$  nanoparticles. (C) The energy dispersive spectrum measured the synthesized nanoparticles.

diameter 86.42 nm) and possess a hexagonal array of pores sized around 2.5 nm with a 5.7 atomic% Gd doping. Gd is present in the form of  $Gd_2O_3$  clusters. The energy-dispersive spectrum (C) of the nanoparticles indicates that Gd atoms are incorporated into the framework of MCM-41 silica.

## Magnetic cell labeling, cell viability, and differentiation

TEM images (Figure 2A) visually confirmed the cellular uptake of  $Gd_2O_3@MCM-41$  nanoparticles, which appear as black pellets enclosed within endosomes and in the cytoplasmic compartment of MSCs. The in vitro detection level by MRI is important to estimate the feasibility of visualizing  $Gd_2O_3@MCM-41$ -labeled cells. As can be seen in Figure 2B, coinubation of MSCs with 50  $\mu g/mL$   $Gd_2O_3@MCM-41$  provided the optimal signal.

In vitro survival and differentiation of the labeled cells were analyzed before the animal experiments were conducted. We first detected the proliferation of labeled MSCs by MTT assay (Figure 2C). There was no significant difference between labeled and unlabeled cells ( $P < 0.05$ ), which suggests that  $Gd_2O_3@MCM-41$  did not significantly affect cell viability and proliferation at the tested concentrations over 12 days in cell culture.

The endogenous differentiation potency of labeled MSCs and NSCs was detected to further evaluate the biocompatibility of  $Gd_2O_3@MCM-41$ . Labeled MSCs (50  $\mu g/mL$ ) were successfully induced to differentiate into adipocytes (lipid droplets were stained with oil red O), osteocytes (alkaline phosphatase activity detected by fast blue RR salt), and chondrocytes (cartilaginous nodules stained by alcian blue), and no apparent discrepancy was observed between labeled MSCs and control cells (Figure 3A). Labeled NSCs displayed typical multipolar neuron morphology (50  $\mu g/mL$ ), similar to the findings in nonlabeled cells (Figure 3B).  $\beta$ -Tubulin III is a characteristic marker of neurons rich in perikaryon and

dendrites of neurons. GFP-positive cells were basically colocalized with  $\beta$ -tubulin cells. Immunoreactivity for  $\beta$ -tubulin III (red) was shown clearly in both groups.

The in vitro results preliminarily indicated that  $Gd_2O_3@MCM-41$  had better cell-tracking ability, and did not affect the viability and differentiation potential of MSCs and NSCs.

## In vivo imaging

We performed MRI for labeled MSCs in the muscle of SD rats (Figure 4A). Labeled cells injected intramuscularly into the left thigh produced a bright area on axial  $T_1$  images (Figure 4A, right). The signal intensity of  $Gd_2O_3@MCM-41$ -labeled MSCs (average signal intensity, 69.3) was increased by 154% on  $T_1$ -weighted images compared to the surrounding muscle (average signal intensity, 45.0).

For labeled NSCs, we examined their trackability in the brain of SD rats. The intracerebral transplants of  $Gd_2O_3@MCM-41$ -labeled NSCs were able to be visualized for a long time – at least 14 days – by 3T MRI. As shown in Figure 4B, labeled NSCs, identified by a hyperintense signal, were found in the sagittal plane 4–14 days after implantation. We noted that on day 4, the MR signal around the injection site was present but not very obvious. On day 9 and day 14, the hyperintensity gradually enlarged and became clear.

Histological examination was conducted to investigate the behavior of donated NSCs, including their survival, differentiation, biodistribution, and migration. It also helped to evaluate the biocompatibility as well as the application of  $Gd_2O_3@MCM-41$ . After final MR scanning, animals were killed for histological analysis. The injection area could be seen clearly in hematoxylin and eosin-stained sections, and many labeled cells with black  $Gd_2O_3@MCM-41$  nanoparticles were observed at the injection site using a high-magnification light microscope (Figure 5A). This was consistent with the aforementioned MR images. Some GFP-expressing labeled

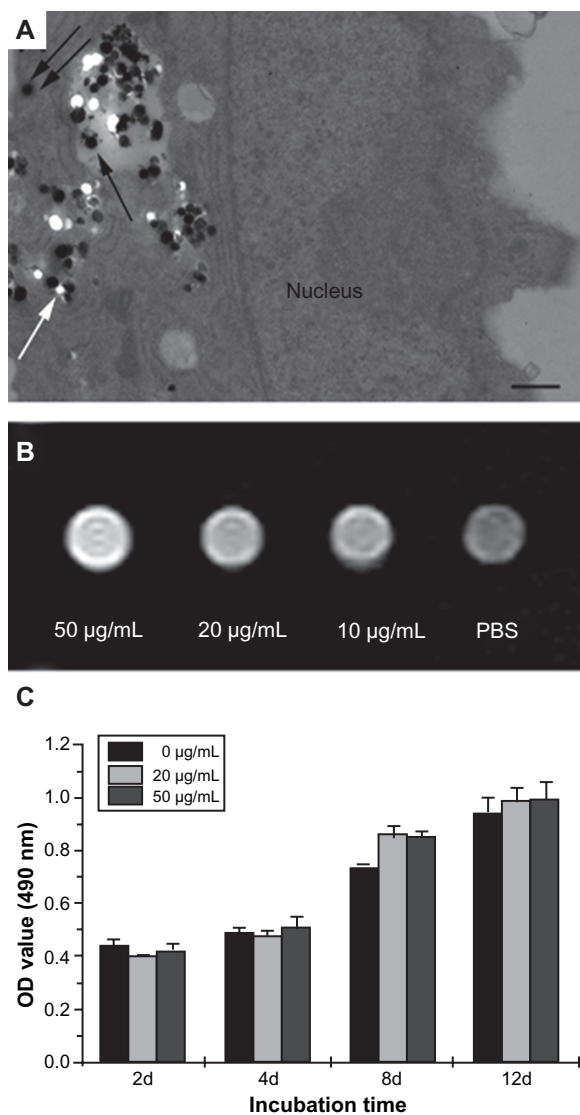


**Figure 2** (A) Transmission electron microscopy images of gadolinium-doped mesoporous silica MCM-41 (Gd<sub>2</sub>O<sub>3</sub>@MCM-41)-labeled mesenchymal stem cells (MSCs). Gd<sub>2</sub>O<sub>3</sub>@MCM-41 nanoparticles are observed as black particles in the secondary lysosome (black arrow) and the cytoplasm (double black arrows). The white spots (white arrow) were the result of the nanoparticles being separated into sections. Scale bar = 500 nm. (B) T<sub>1</sub>-weighted magnetic resonance image of MSCs incubated with Gd<sub>2</sub>O<sub>3</sub>@MCM-41 at different concentrations (50, 20, and 10 μg/mL). (C) The proliferation of Gd<sub>2</sub>O<sub>3</sub>@MCM-41-labeled MSCs at different concentrations (50 and 20 μg/mL) and non-labeled MSCs by MTT assay after 2, 4, 8, and 12 days of treatment.

**Abbreviations:** PBS, phosphate-buffered saline; OD, optical density; MTT, 3-(4,5-dimethylthiazol-2-yl)-2,5-diphenyltetrazolium bromide.

NSCs (green) showed immunoreactivity for β-tubulin III (red) and had a typical multipolar neuron morphology; this means that both Gd<sub>2</sub>O<sub>3</sub>@MCM-41-labeled NSCs and unlabeled NSCs grafted into the brain were able to differentiate into neuron-like cells (Figure 5C).

## Discussion

Gd<sub>2</sub>O<sub>3</sub>@MCM-41 as a stem cell tracer needs to be investigated for its effects on the behavior of cells, including cell survival

and differentiation, in vitro before animal experimentation. The Gd<sub>2</sub>O<sub>3</sub>@MCM-41 nanoparticles in the labeled cells still remained in pellet form and were monodispersed without cluster formation, as seen in the TEM images (Figure 2A), which was in agreement with the results for Gd<sub>2</sub>O<sub>3</sub>@MCM-41 nanoparticles (Figure 1A). The nanoparticles were taken up via endocytosis and formed vesicles in cells. Some Gd<sub>2</sub>O<sub>3</sub>@MCM-41 nanoparticles in vesicles were transported into the cytoplasm. During the process of making the slide, some nanoparticles in vesicles may have been moved out and appeared in the cytoplasm, which explains the nanoparticles being observed there. MTT assay suggested that Gd<sub>2</sub>O<sub>3</sub>@MCM-41 did not significantly affect cell proliferation at the tested concentrations (0, 20, and 50 μg/mL) over 12 days. The 50 μg/mL concentration showed obvious contrast enhancement (Figure 2B) and satisfied the requirements for cell tracing. Despite this finding, we think that it is not necessary to use more nanoparticles to label cells, since they are considered as foreign bodies by cells. Besides, in the pilot experiments (data not shown), we found that the high concentration decreased the dispersibility of nanoparticles, leading to poor imaging results. Tseng et al pointed out that when the concentration of Gd is too high, the effect of T<sub>2</sub> relaxation will overcome the effect of T<sub>1</sub> and this will suppress the T<sub>1</sub> signal.<sup>8</sup> The nanoparticles could remain in the cells for several days; for example, the cells prelabeled with nanoparticles for 7 days could still be detected by MRI.<sup>21</sup>

Stem cells are functionally defined by their capacity for self-renewal and differentiation into multiple cell types. MSCs can differentiate into various types of cells under various conditions, such as adipocytes, osteocytes, chondrocytes, and neurons.<sup>26</sup> After culture for 2–3 weeks under appropriate conditions for differentiation, labeled MSCs (50 μg/mL) also grew normally and could successfully differentiate into adipocytes, osteocytes, and chondrocytes, similar to the findings in the nonlabeled cells (Figure 3A). NSCs also have the ability to differentiate into neurons of all types, astrocytes of all types, and oligodendrocytes.<sup>27</sup> Neuronal differentiation of NSCs could be promoted by genetically enhanced expression of NT-3 and its high-affinity receptor tyrosine kinase receptor C.<sup>3</sup> NT-3-NSCs and tyrosine kinase receptor C-NSCs were mixed in a 1:1 proportion and cultured together, which increased neuronal differentiation of labeled NSCs as well as control cells (Figure 3B). We selected one or more representative inducing conditions for the two cells to show that Gd<sub>2</sub>O<sub>3</sub>@MCM-41 affects differentiation only to a small extent. The results of the in vitro experiments showed that it was possible to transplant them into animals.

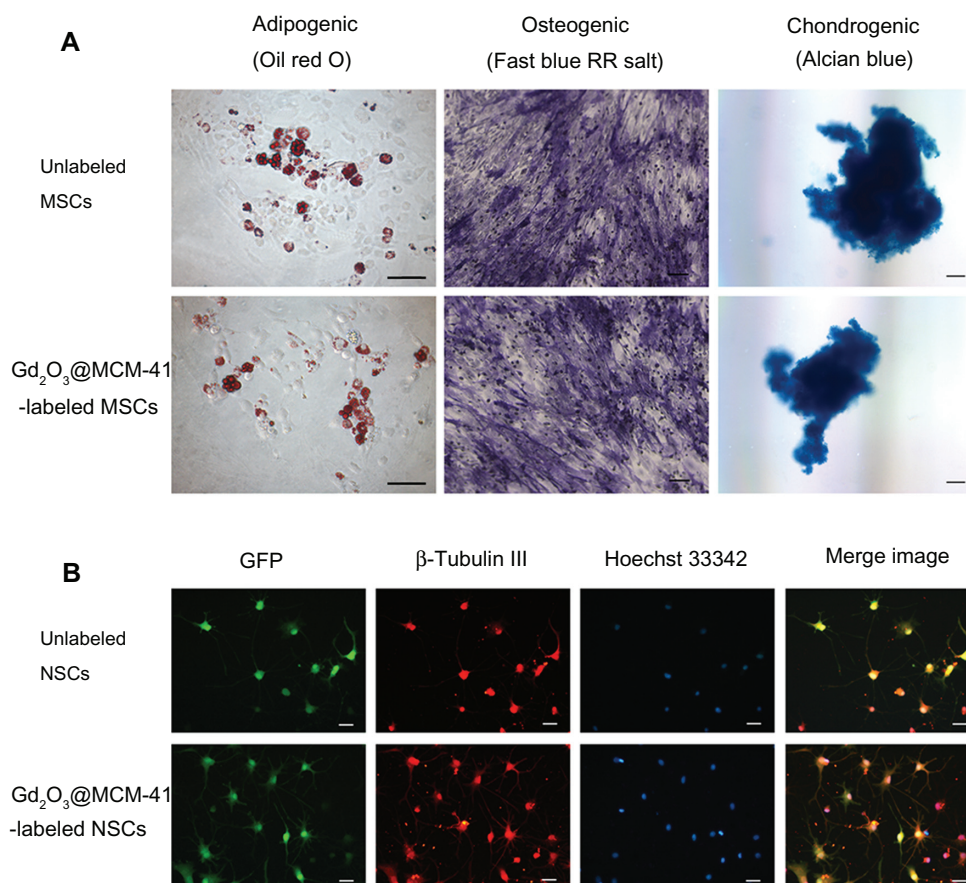


**Figure 3** (A) Adipogenic, osteogenic, and chondrogenic differentiation of unlabeled and gadolinium-doped mesoporous silica MCM-41 ( $Gd_2O_3@MCM-41$ )-labeled mesenchymal stem cells (MSCs). (B) Immunocytochemical staining of neuronal differentiation ( $\beta$ -tubulin III, red) and nuclear staining (Hoechst 33342, blue) of unlabeled and  $Gd_2O_3@MCM-41$  labeled green fluorescent protein (GFP)-expressing neural stem cells (NSCs) (green). Scale bars: (A) 100  $\mu m$ , (B) 25  $\mu m$ .

$Gd_2O_3@MCM-41$  as a positive cellular tracer produced bright signals in  $T_1$ -weighted MR images and was superior to negative contrast agents, such as SPIO, especially in the case of hypointense tissues. In the animal experiment, the hemorrhage in the injured rat brain caused by the microsyringe was unavoidable during the transplantation surgery. The low hemorrhage signal might puzzle researchers with regard to distinguishing between the donated SPIO-labeled cells and the surrounding tissue. On the contrary, the hyperintensity produced by  $Gd_2O_3@MCM-41$  in  $T_1$ -weighted MR images aided in identifying the location of the labeled NSCs more effectively, while the injection area with a low MR signal was clearly observed. Therefore, it can be concluded that  $Gd_2O_3@MCM-41$  can provide accurate tracking information and is suited for application in vivo.

Cell transplantation as a method of stem cell therapy has gained widespread attention in biomedicine.<sup>26</sup> However, the amount of stem cells transplanted into the body is relatively small, so a highly sensitive tracking technique is

required to detect these cells in the body.  $Gd_2O_3@MCM-41$  nanoparticles can carry high  $Gd^{3+}$  payloads and facilitate greater interaction between protons and Gd ions, indicating that lower amounts of the agent are needed to produce the desired contrast. In our in vivo assay, MSCs were labeled with  $Gd_2O_3@MCM-41$  (50  $\mu g/mL$ ) and implanted into the muscles of SD rats.  $T_1$ -weighted images (at 3 T) showed high contrast (Figure 4A, right), indicating the high sensitivity of  $Gd_2O_3@MCM-41$  as a cellular MR tracer. A greater amount of MSCs was injected into muscle ( $4 \times 10^6$ ) than into the brain ( $1 \times 10^5$ ); therefore, a bright signal could be seen at day 1. Unfortunately, rat muscle has a high metabolic rate, which made it difficult to trace the labeled MSCs for a long time. Besides, we have demonstrated that labeled MSCs retain their differentiation potential in vitro; whether this is the case in vivo needs to be investigated in future studies. Recent research suggests that MSCs play an important role in mending damaged tissue, owing to their high self-renewal capacity and potential to differentiate into many

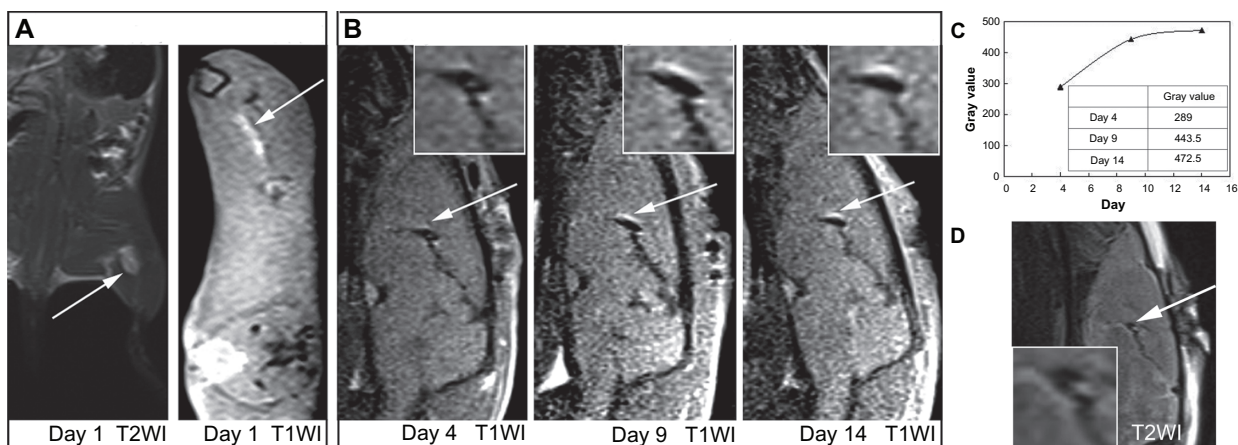


**Figure 4** (A) Magnetic resonance (MR) images of gadolinium-doped mesoporous silica MCM-4I (Gd<sub>2</sub>O<sub>3</sub>@MCM-4I)-labeled mesenchymal stem cells ( $4 \times 10^6$ , 50  $\mu$ g Gd<sub>2</sub>O<sub>3</sub>@MCM-4I/mL) injected into the rat thigh at 3.0 T. (B) Serial T<sub>1</sub>-weighted MR images of Gd<sub>2</sub>O<sub>3</sub>@MCM-4I labeled neural stem cells ( $1 \times 10^5$ , 50  $\mu$ g Gd<sub>2</sub>O<sub>3</sub>@MCM-4I/mL) injected into the rat brain on day 4, day 9, and day 14 at 3.0 T. Arrows mark the injection site. (C) The time-increased signal of (B). (D) T<sub>2</sub>-weighted MR image on day 4 showed that the signal did not come from hemorrhage.

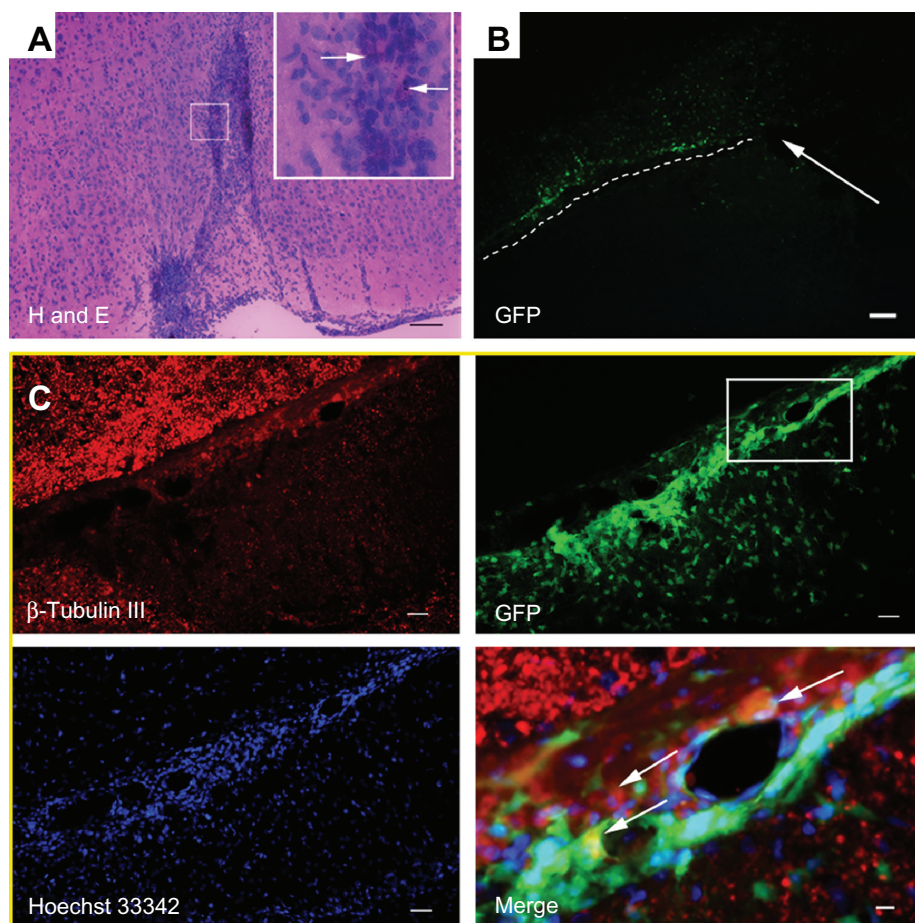


**Figure 5** (A–C) Brains of the rats were removed at 15 days posttransplantation. (A) Hematoxylin and eosin-stained sections of the rat brain. The injection site of gadolinium-doped mesoporous silica MCM-4I (Gd<sub>2</sub>O<sub>3</sub>@MCM-4I)-labeled neural stem cells (NSCs) is displayed, and arrows mark the black Gd<sub>2</sub>O<sub>3</sub>@MCM-4I nanoparticles in cells. (B) Green fluorescent protein (GFP)-expressing Gd<sub>2</sub>O<sub>3</sub>@MCM-4I labeled NSCs in the brain were clearly seen. The injection area is marked with a white arrow and the migration of Gd<sub>2</sub>O<sub>3</sub>@MCM-4I-labeled NSCs is shown by the white dotted line. (C)  $\beta$ -tubulin III (red) and Hoechst 33342 (blue) staining for GFP-expressing Gd<sub>2</sub>O<sub>3</sub>@MCM-4I labeled NSCs (green). The area in the white box in the GFP image is magnified in the Merge image. Donated NSCs (green) showed immunoreactivity for  $\beta$ -tubulin III (red) and Hoechst 33342 nuclear staining (blue), shown by white arrows in the Merge image. Scale bars: (A) 100  $\mu$ m, (B) 80  $\mu$ m, (C) 100  $\mu$ m (except Merge image: 25  $\mu$ m).

cell types. Further studies should be conducted to monitor the fate of transplanted labeled MSCs in therapeutic models of animals.

In addition, we noted that the bright-signal areas indicating labeled NSCs migrated gradually from the grafted area to the ventral part of the brain. The hyperintensity produced by  $Gd_2O_3@MCM-41$  was enhanced with increase in time. On day 4, the positive Gd signal was not obvious. On day 9 and day 14, hyperintensity was gradually enlarged and became clear (Figure 4B). Only a small amount of NSCs ( $1 \times 10^5$ ) were injected into the brain, to ensure survival of the animals; because of this and the dilution of PBS and tissue edema, the early MRI signal was not obvious. With increase in time, PBS was absorbed gradually by the surrounding tissue and the early inflammatory reaction dissipated,<sup>15</sup> resulting in significant signal enhancement in  $T_1$ -weighted MR images. Clear migration of labeled NSCs identified by MRI from the injection area was observed better in the immunofluorescent images (Figure 5B). Jandial et al reported that NSCs possessed the inherent properties of long-distance migration.<sup>27</sup> Donated NSCs preferentially gathered close gradually toward the lesion area, which indicates that they might play a role in rodent tissue repair. These properties can be exploited for cell therapies for neurologic diseases. Histological analyses after 14 days of tracking suggested that labeled NSCs retained their neuronal differentiation potential in murine models, from which it could be concluded that  $Gd_2O_3@MCM-41$  was suitable for tracking stem cells in the therapy model. Though during the long-term migration, all the labeled NSCs might not have survived and some nanoparticles might have leaked or been phagocytosed, most of the donated cells had survived and retained their capacity for neuronal differentiation. This suggests that  $Gd_2O_3@MCM-41$  is less toxic as a stem cell tracer when transplanted; more detailed studies on its biological toxicity in vivo are expected at the next stage of the experiment.

## Acknowledgments

This work was supported by grants from the National Natural Science Foundation of China (numbers 81071207, 10875178, and 81271622), and the Fundamental Research Funds for the Central Universities (no 10ykjcll).

## Disclosure

The authors report no conflicts of interest in this work.

## References

- Phinney DG, Prockop DJ. Concise review: mesenchymal stem/multipotent stromal cells: the state of transdifferentiation and modes of tissue repair – current views. *Stem Cells*. 2007;25:2896–2902.
- Kurozumi K, Nakamura K, Tamiya T, et al. Mesenchymal stem cells that produce neurotrophic factors reduce ischemic damage in the rat middle cerebral artery occlusion model. *Mol Ther*. 2004;11:96–104.
- Wang JM, Zeng YS, Wu JL, Li Y, Teng YD. Cograft of neural stem cells and Schwann cells overexpressing TrkC and neurotrophin-3 respectively after rat spinal cord transection. *Biomaterials*. 2011;32:7454–7468.
- Cao Q, Benton RL, Whittemore SR. Stem cell repair of central nervous system injury. *J Neurosci Res*. 2002;68:501–510.
- Einstein O, Ben-Hur T. The changing face of neural stem cell therapy in neurologic diseases. *Arch Neurol*. 2008;65:452–456.
- Park KI, Himes BT, Stieg PE, Tessler A, Fischer I, Snyder EY. Neural stem cells may be uniquely suited for combined gene therapy and cell replacement: evidence from engraftment of neurotrophin-3-expressing stem cells in hypoxic-ischemic brain injury. *Exp Neurol*. 2006;199:179–190.
- Sun C, Lee JSH, Zhang M. Magnetic nanoparticles in MR imaging and drug delivery. *Adv Drug Deliver Rev*. 2008;60:1252–1265.
- Tseng CL, Shih IL, Stobinski L, Lin FH. Gadolinium hexanedione nanoparticles for stem cell labeling and tracking via magnetic resonance imaging. *Biomaterials*. 2010;31:5427–5435.
- Yang H, Zhuang Y, Sun Y, et al. Targeted dual-contrast T1- and T2-weighted magnetic resonance imaging of tumors using multifunctional gadolinium-labeled superparamagnetic iron oxide nanoparticles. *Biomaterials*. 2011;32:4584–4593.
- Tran LA, Krishnamurthy R, Muthupillai R, et al. Gadonanotubes as magnetic nanolabels for stem cell detection. *Biomaterials*. 2010;31:9482–9491.
- Marquis BJ, Love SA, Braun KL, Haynes CL. Analytical methods to assess nanoparticle toxicity. *Analyst*. 2009;134:425–439.
- Anderson SA, Lee KK, Frank JA. Gadolinium-fullerenol as a paramagnetic contrast agent for cellular imaging. *Invest Radiol*. 2006;41:332–338.
- Rogers WJ, Meyer CH, Kramer CM. Technology insight: in vivo cell tracking by use of MRI. *Nat Clin Pract Cardiovasc Med*. 2006;3:554–562.
- Modo M, Cash D, Mellodew K, et al. Tracking transplanted stem cell migration using bifunctional, contrast agent-enhanced, magnetic resonance imaging. *Neuroimage*. 2002;17:803–811.
- Chen A, Siow B, Blamire AM, Lako M, Clowry GJ. Transplantation of magnetically labeled mesenchymal stem cells in a model of perinatal brain injury. *Stem Cell Res*. 2010;5:255–266.
- Henning TD, Saborowski O, Golovko D, et al. Cell labeling with the positive MR contrast agent gadofluorine M. *Eur Radiol*. 2007;17:1226–1234.
- Lin YS, Hung Y, Su JK, et al. Gadolinium(III)-incorporated nanosized mesoporous silica as potential magnetic resonance imaging contrast agents. *J Phys Chem B*. 2004;108:15608–15611.
- Li S, Liu H, Li L, et al. Mesoporous silica nanoparticles encapsulating  $Gd_2O_3$  as a highly efficient magnetic resonance imaging contrast agent. *Appl Phys Lett*. 2011;98:093704.
- Hahn MA, Singh AK, Sharma P, Brown SC, Moudgil BM. Nanoparticles as contrast agents for in-vivo bioimaging: current status and future perspectives. *Anal Bioanal Chem*. 2011;399:3–27.
- Huang CC, Liu TY, Su CH, Lo YW, Chen JH, Yeh SC. Superparamagnetic hollow and paramagnetic porous  $Gd_2O_3$  particles. *Chem Mater*. 2008;20:3840–3848.
- Hsiao JK, Tsai CP, Chung TH, et al. Mesoporous silica nanoparticles as a delivery system of gadolinium for effective human stem cell tracking. *Small*. 2008;4:1445–1452.

22. Shao YZ, Liu LZ, Song SQ, et al. A novel one-step synthesis of Gd<sup>3+</sup>-incorporated mesoporous SiO<sub>2</sub> nanoparticles for use as an efficient MRI contrast agent. *Contrast Media Mol Imaging*. 2010;6:110–118.
23. Miyawaki J, Yudasaka M, Imai H, et al. Synthesis of ultrafine Gd<sub>2</sub>O<sub>3</sub> nanoparticles inside single-wall carbon nanohorns. *J Phys Chem B*. 2006;110:5179–5181.
24. Park JY, Baek MJ, Choi ES, et al. Paramagnetic ultrasmall gadolinium oxide nanoparticles as advanced T1 MRI contrast agent: account for large longitudinal relaxivity, optimal particle diameter, and in vivo T1 MR images. *ACS Nano*. 2009;3:3663–3669.
25. Shao YZ, Tian XM, Hu WY, et al. The properties of Gd<sub>2</sub>O<sub>3</sub>-assembled silica nanocomposite targeted nanoprobes and their application in MRI. *Biomaterials*. 2012;33:6438–6446.
26. Zhang W, Yan Q, Zeng YS, et al. Implantation of adult bone marrow-derived mesenchymal stem cells transfected with the neurotrophin-3 gene and pretreated with retinoic acid in completely transected spinal cord. *Brain Res*. 2010;1359:256–271.
27. Jandial R, Singec I, Ames CP, Snyder EY. Genetic modification of neural stem cells. *Mol Ther*. 2008;16:450–457.

### International Journal of Nanomedicine

### Publish your work in this journal

The International Journal of Nanomedicine is an international, peer-reviewed journal focusing on the application of nanotechnology in diagnostics, therapeutics, and drug delivery systems throughout the biomedical field. This journal is indexed on PubMed Central, MedLine, CAS, SciSearch®, Current Contents®/Clinical Medicine,

Submit your manuscript here: <http://www.dovepress.com/international-journal-of-nanomedicine-journal>

Journal Citation Reports/Science Edition, EMBase, Scopus and the Elsevier Bibliographic databases. The manuscript management system is completely online and includes a very quick and fair peer-review system, which is all easy to use. Visit <http://www.dovepress.com/testimonials.php> to read real quotes from published authors.

Dovepress